



# Self-organization in the spatial battle of the sexes with probabilistic updating

Ramón Alonso-Sanz\*

Polytechnic University of Madrid, ETSI Agrónomos (Estadística, GSC), C. Universitaria. 28040, Madrid, Spain

---

## ARTICLE INFO

### Article history:

Received 30 September 2010

Received in revised form 21 March 2011

Available online 13 April 2011

### Keywords:

Battle of sexes

Spatial

Probabilistic

Memory

---

## ABSTRACT

The dynamics of a spatial formulation of the iterated battle of the sexes with probabilistic updating is assessed in this work. The game is played in the cellular automata manner, i.e., with local and synchronous interaction. The effect of memory of past encounters is also taken into account. It is concluded that the spatial structure enables the emergence of clusters of coincident choices, leading to the mean payoff per encounter to values that are accessible only in the cooperative two-person game scenario, which constitutes a notable case of self-organization. With probabilistic updating of choices, both kinds of players reach mean payoffs per encounter that are notably higher than those reached with a deterministic updating mechanism, albeit the evolutionary dynamics does not stabilize, and one of the two possible choices tends to prevail for both kinds of players. Memory of past iterations induces an inertial effect that moderates this tendency, so that intermediate levels of the memory charge tend to favor fairly stable high egalitarian payoffs, without impeding the necessary recovering from their initial plummeting.

© 2011 Elsevier B.V. All rights reserved.

---

## 1. Introduction

The so called *battle of the sexes* (BOS for short) is a simple example of a two-person asymmetric game [1,2]. In this game, the preferences of a conventional couple are assumed to fit the traditional stereotypes: the male prefers to attend a Football match, whereas the female prefers to attend a Ballet performance. Both players (which are treated symmetrically), decide in the hope of getting together, so that their payoff matrices are given in the far left panel of Table 1, with rewards  $R > r > 0$ . Thus, the expected payoffs ( $p$ ) in the BOS game, using uncorrelated mixed probabilistic strategies  $(x, 1 - x)$  and  $(y, 1 - y)$  are:

$$p_{\sigma}(x; y) = (x, 1 - x) \begin{pmatrix} R & 0 \\ 0 & r \end{pmatrix} \begin{pmatrix} y \\ 1 - y \end{pmatrix} = ((R + r)y - r)x + r(1 - y) \quad (1)$$

$$p_{\varphi}(y; x) = (x, 1 - x) \begin{pmatrix} r & 0 \\ 0 & R \end{pmatrix} \begin{pmatrix} y \\ 1 - y \end{pmatrix} = ((R + r)x - R)y + R(1 - x). \quad (2)$$

In game theory, the best response is the strategy (or strategies) which produces the most favorable outcome for a player, taking other players' strategies as given. Best response correspondences, also known as reaction functions, can be drawn for all  $2 \times 2$  normal form games with a line for each player in a unit square strategy space as shown in the central panel of Table 1, in which vertical/horizontal lines indicate no definition. The pair of strategies  $((x, 1 - x), (y, 1 - y))$ , are in Nash

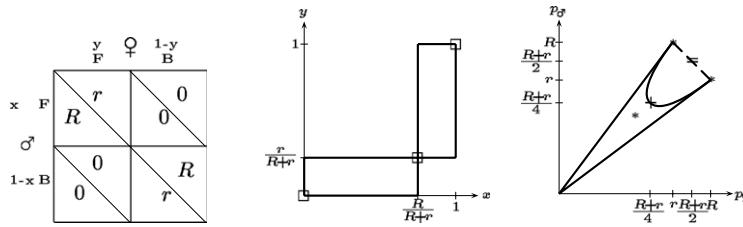
---

\* Tel.: +34 91 3365871.

E-mail address: [ramon.alonso@upm.es](mailto:ramon.alonso@upm.es).

**Table 1**

The payoff matrices (left), reaction correspondences (center) and payoff region (right) in the *battle of the sexes* game.



equilibrium if  $x$  is a best response to  $y$  and  $y$  is a best response to  $x$ . Thus, no player can benefit from changing his strategy while the other keeps his unchanged. Formally:  $p_A(x, y) \geq p_A(z, y)$ , and  $p_B(x, y) \geq p_B(x, z)$ ,  $\forall z$ . Nash equilibria are shown with points where the two player's correspondences agree, i.e. cross, in the reaction correspondence graphs. Thus, according to the reaction correspondences given in Table 1, the pairs of strategies in Nash equilibrium are, the pure  $(0, 0)$  and  $(1, 1)$ , and the mixed  $(x^* = R/(R+r), y^* = r/(R+r))$ . In the latter, every player assigns to his preferred option (the same) higher probability, i.e.,  $x^* = 1 - y^*$ . It is,  $p_\sigma(x^*, y^*) = p_\varphi(x^*, y^*) = rR/(R+r) < r < R$ , i.e., the geometric mean of  $R$  and  $r$ . Pareto-efficient situations are those in which it is impossible to make one player better off without necessarily making someone else worse off. Thus, only the two pure Nash equilibrium strategies (also termed *coordinated*) are Pareto efficient.

Both players get the same payoff if  $y = 1 - x$ , in which case,  $p = (R + r)(1 - x)x$ . This egalitarian payoff is maximum when  $x = y = 1/2$ , with  $p^+ = (R + r)/4$ , the point marked + in the far right panel of Table 1. Thus, the set of payoffs which can be obtained by both players (or payoff region) is closed by the parabola passing by  $(R, r)$ ,  $(r, R)$ , and  $(p^+, p^+)$ , as shown in the payoff region panel of Table 1. Incidentally, in most games the payoff region is easier to draw, as its boundaries are obtained just by considering the *extreme* parameter values  $x = 0, x = 1, y = 0, y = 1$ . This is not so in the BOS, where only the linear segments of the payoff region are obtained in this way.<sup>1</sup>

In a broader game scenario, a probability distribution  $A = (a_{ij})$  assigns probability to every combination of player choices, so  $A = \begin{pmatrix} a_{11} & a_{12} \\ a_{21} & a_{22} \end{pmatrix}$  in  $2 \times 2$  games [3]. Thus, the expected payoffs in the BOS are:  $\frac{p_\sigma}{p_\varphi} = \frac{a_{11}R + a_{22}r}{a_{11}r + a_{22}R}$ . The probability distribution (strategy)  $A = (a_{ij})$  is in *correlated equilibrium* [4,5] if the players cannot gain by disobeying the signals given by the randomization device  $A$ . Thus, for example, in the BOS if the male player is given the  $F$  signal, by obeying it the  $\sigma$ -player gets:  $p_\sigma/F = a_{11}R/(a_{11} + a_{12})$ , whereas disobeying his mean payoff is:  $a_{12}r/(a_{11} + a_{12})$ , and correlated equilibrium demands  $a_{11}R \geq a_{12}r$ . Analogously,  $p_\sigma/B = a_{22}r/(a_{21} + a_{22}) \geq a_{21}R/(a_{21} + a_{22}) \rightarrow a_{22}r \geq a_{21}R$ ;  $p_\varphi/F = a_{11}r/(a_{11} + a_{21}) \geq a_{21}R/(a_{11} + a_{21}) \rightarrow a_{11}r \geq a_{21}R$ ;  $p_\sigma/B = a_{22}R/(a_{12} + a_{22}) \geq a_{12}r/(a_{12} + a_{22}) \rightarrow a_{22}R \geq a_{12}r$ . If  $a_{12} = a_{21} = 0$  every former inequality holds, i.e.,  $a_{11}R \geq 0$ ,  $a_{22}r \geq 0$ ,  $a_{11}r \geq 0$ , and  $a_{22}R \geq 0$ , so that  $A = \begin{pmatrix} a & 0 \\ 0 & 1-a \end{pmatrix}$  is in correlated equilibrium, giving:  $\frac{p_\sigma}{p_\varphi} = ar + (1-a)r$ , so a convex  $(0 \leq a \leq 1)$  combination of the  $(R, r)$  and  $(r, R)$  points, i.e., the segment that joins these points in the payoff region. Now the payoff region limited by the parabola and the segment that joins the Pareto optimal pairs of payoffs becomes accessible. In this scenario both players reach a maximum egalitarian payoff  $p^+ = (R + r)/2$  (the point marked = in the payoff region of Table 1), with  $a = 1/2$ , i.e., fully discarding the mutually inconvenient  $FB$  and  $BF$  combinations and adopting  $FF$  and  $BB$  with equal probability.

Correlation, namely *entanglement*, is in the core of quantum theory, thus in quantum games [6], and consequently in the quantum approach to the battle of the sexes [7,8].

## 2. The spatialized battle of the sexes: deterministic updating

In the spatial version of the BOS cellular automaton we dealt with, each player occupies a site  $(i, j)$  in a two-dimensional  $N \times N$  lattice. We will consider that *males* and *females* alternate in the site occupation, so that in the chessboard form shown in the far left panel of Table 2, every player is surrounded by four partners ( $\varphi-\sigma$ ,  $\sigma-\varphi$ ), and four mates ( $\varphi-\varphi$ ,  $\sigma-\sigma$ ).

In a CA-like implementation, in each generation ( $T$ ) every player plays with his four adjacent partners, so that the payoff of a given individual ( $p_{i,j}^{(T)}$ ), is the sum over these four interactions. In the next generation, every player will adopt the choice ( $d_{i,j}^{(T)}$ ) of his nearest-neighbor mate (including himself) that received the highest payoff. In case of a tie, the player maintains his choice.

<sup>1</sup>  $x = 0 \rightarrow \begin{cases} p_\sigma = r(1-y) \\ p_\varphi = R(1-y) \end{cases}$ , so a convex  $(0 \leq y \leq 1)$  combination of the  $(R, r)$  and  $(0, 0)$  points;  $y = 0 \rightarrow \begin{cases} p_\sigma = r(1-x) \\ p_\varphi = R(1-x) \end{cases}$ , which again defines the boundary segment  $(R, r) - (0, 0)$ ;  $x = 1 \rightarrow \begin{cases} p_\sigma = Ry \\ p_\varphi = ry \end{cases}$ , which defines the boundary segment  $(r, R) - (0, 0)$ ;  $y = 1 \rightarrow \begin{cases} p_\sigma = Rx \\ p_\varphi = rx \end{cases}$ , again the boundary segment  $(r, R) - (0, 0)$ .

**Table 2**

The battle of the sexes cellular automaton.  $R = 5$ ,  $r = 1$ .

	$T = 1$	$T = 2$
$\sigma$	$F B F B F B F B$	$F B F B F B F B$
$\varphi$	$B F B F B F B F$	$B F B F B F B F$
$\sigma$	$F B F B F B F B$	$F B B B B B F B$
$\varphi$	$B F B B B F B F$	$B F B B B F B F$
$\sigma$	$F B F B F B F B$	$F B B B B B F B$
$\varphi$	$B F B F B F B F$	$B F B F B F B F$
$\sigma$	$F B F B F B F B$	$F B F B F B F B$
$\varphi$	$B F B F B F B F$	$B F B F B F B F$

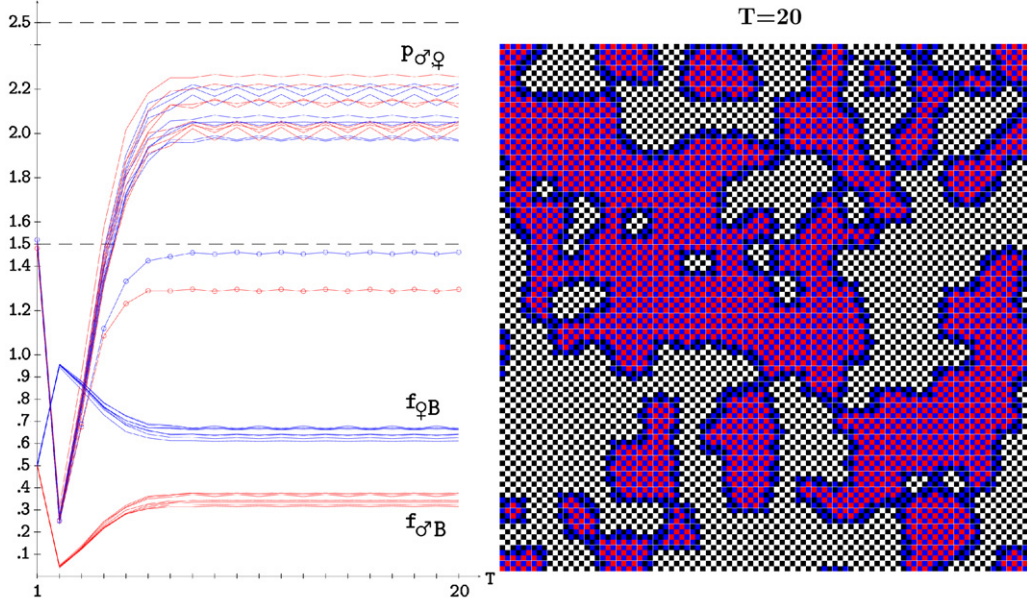


**Fig. 1.** Left: The ballet frequency ( $f$ ) and mean payoff per encounter ( $p$ ) in nine simulations in the deterministic ( $R = 5$ ,  $r = 1$ ) BOS cellular automaton. All the simulations are run in a  $100 \times 100$  lattice with periodic boundary conditions. Right: The pattern at  $T = 20$  of a simulation. (For interpretation of the references to colour in this figure legend, the reader is referred to the web version of this article.)

In the initial scenario of Table 2, every player chooses his preferred choice, except a male in the central part of the lattice that chooses *ballet*. As a result, the general income is nil with the only exception arising from the  $\sigma$ -ballet choice. This reports four units (assuming  $r = 1$ ) to the initial *deviated* male, and fires the change to *ballet* of the four males connected with the initial  $\sigma$ -ballet as indicated under  $T = 2$  in Table 2. The change  $\sigma$ -football to  $\sigma$ -ballet advances in this way at every time-step, so that in this simple example every player will choose *ballet* in the long term.

The ballet frequency and mean payoff per encounter ( $p$ ) in the ( $R = 5$ ,  $r = 1$ ) BOS cellular automaton starting from nine random initial configurations of choices are shown in the left panel of Fig. 1. Initially, as a result of the random assignment of choices, the  $B$ -frequencies (and that of  $F$ ) are 0.5, and the mean payoffs commence at the arithmetic mean of the payoff values, i.e.,  $p^+ = (R + r)/4 = 1.5$ .

After the first round, both types of players drift to their preferred choice, and as consequence both payoffs plummet at  $T = 2$ . But immediately such a drift becomes moderated, and both  $p$  recover. In the long-term the  $B$ -frequencies stabilize at values that are not off from the  $B$ -probabilities in the mixed equilibrium strategy of a two-person game:  $1 - x^* = r/(R + r) = 0.17$ ,  $1 - y^* = R/(R + r) = 0.83$ .

The dotted curves in the left panel of Fig. 1 show, in one of the simulations, the *theoretical* payoffs of both players in a two-person game with independent strategies using as probabilities the evolving frequencies, namely:

$$p_{\sigma}^{(T)} = ((R + r)(1 - f_{\varphi B}) - r)(1 - f_{\sigma B}) + r f_{\varphi B}, \quad (3)$$

$$p_{\varphi}^{(T)} = ((R + r)(1 - f_{\sigma B}) - R)(1 - f_{\varphi B}) + R f_{\sigma B}. \quad (4)$$

The actual mean payoffs of both kinds of players shown in Fig. 1 are over these *expected* values due to the spatial structure, which allows for the emergence of clusters of *agreement*, shown in the right panel of Fig. 1 as black-white (FF) and red-blue (BB) regions with interfaces of disagreement among the clusters.

The study of spatial games was pioneered by Nowak and May [9,10] with regards to the Prisoner's Dilemma (PD) [11]. They concluded in their original work that spatial structure (or territoriality) can facilitate the survival of cooperators. Thus, the spatialized PD has proved to be a promising tool to explain how cooperation can hold out against the ever-present threat of exploitation. The notable case of self-organization in the BOS just presented appears as a novel example of the boosting effect induced by the spatial ordered structure, which allows access to payoffs which are feasible only with correlated strategies in the two-person game.

Although involving  $N \times N$  players, in the simulations considered in this study pairs of individuals interact in the 2-player, 2-strategy manner. Thus, we are not dealing with an n-person game, were all individuals of the group interact simultaneously. The n-person BOS game has been studied in [12,13]. These studies consider four different payoff functions, modeled as functions of the number of players with the same choice, in a random environment, namely with no spatial structure of player interactions. Our cellular automata-like approach dramatically differs from the context assumed in [12,13], so that the comparison of the results found in [12,13] and those reported here is not feasible.

### 3. Probabilistic updating

In the probabilistic updating mechanism considered from this section, the individuals will play  $F$  or  $B$  with a probability proportional to the total payoff of  $F$  and  $B$  among their mate neighbors. Thus, denoting by  $\mathcal{N}_i$  the mate neighborhood of the generic cell  $i$ , the probabilities that it is occupied by an  $F$ - and  $B$ -player at time-step  $T + 1$  are

$$P(d_i^{(T+1)} = F) = \frac{\sum_{j \in \mathcal{N}_i / d_j^{(T)} = F} p_j^{(T)m}}{\sum_{j \in \mathcal{N}_i} p_j^{(T)m}}, \quad P(d_i^{(T+1)} = B) = 1 - P(d_i^{(T)} = F). \quad (5)$$

The weighting factor  $m$  favors the most successful mate neighbor: the larger  $m$ , the more likely is it that the cell will adopt the strategy of the most successful mate neighbor. We adopt here  $m = 1.0$  (no weighting).

**Fig. 2** shows the initial patterns in the ( $R = 5$ ,  $r = 1$ ) probabilistic BOS cellular automaton in a simulation run in a  $100 \times 100$  lattice size. The evolution of the ballet frequency and mean payoff per encounter starting at random as in the nine simulations of **Fig. 1** is shown in **Fig. 3** up to  $T = 1000$ . The initial patterns in **Fig. 2** correspond to the top-left frame of **Fig. 3**.

After the first round, both types of players drift to their preferred choice in the probabilistic simulations of **Fig. 3** as happened in the deterministic simulations in **Fig. 1**, but to a lower degree. Thus, in **Fig. 1** both  $f_{\sigma^F}$  and  $f_{\sigma^B}$  are over 0.9, whereas in **Fig. 3** these initial frequencies reach levels lower than 0.8.

After the first iteration, the frequencies of both types of choices tend to converge, as indicated in **Fig. 3** in the *Ballet* case, where both  $f_{\sigma^B}$  and  $f_{\sigma^F}$  are almost coincident after the initial transition period, though with  $f_{\sigma^B}$  always over  $f_{\sigma^F}$ . This trend to the  $B$  and  $F$  frequencies converging in both types of players is completely absent in the deterministic model, where the frequencies are soon stabilized in rather different values as shown in **Fig. 1** for the *Ballet* case. Although the way in which the frequencies evolve is fairly monotone, either increasing or decreasing, this is not necessarily so, as the tendency may be inverted. Thus, the simulations labeled 1, 2 and 4 in **Fig. 3** show fairly early swifts in the  $f$ -tendencies, that are marked by a relatively early cross in the mean payoff curves of simulations 1 and 2, whereas in the simulation labeled 4 the  $p$ -cross is reached very late, nearly  $T = 1000$ .

**Fig. 4** shows the patterns at  $T = 100, 200, 500$  and  $1000$  in the nine probabilistic simulations of **Fig. 3**. The agreement clusters are already formed at  $T = 100$ , and in most simulations indicate the long-term dynamics. Thus for example, the central snapshot in every frame, corresponding to the simulation labeled 5 in **Fig. 3**, shows the expansion of the red-blue (BB) cluster, which is already predominant at  $T = 100$ . In the same vein, the bottom-center snapshot in every frame (simulation 8 in **Fig. 3**), shows the expansion of the black-white (FF) region, already predominant at  $T = 100$ , in this case up to the total lattice occupation at  $T = 1000$ . As noted above, this kind of monotone dynamics is not a universal rule, and the (slightly) predominant clusters at  $T = 100$  in the top-left and top-central snapshots (simulations 1 and 2 in **Fig. 3**), are not predominant in the long-term evolution.

As a rule, the drift to one of the choices turns out much faster in small lattices. Thus for example, in two of the three simulations in **Fig. 5** the lattice is soon fully occupied, either by  $B$  in the far left frame, or by  $F$  in the far right frame. But the trend to fast full occupation is not universal, as shows the simulation in the central frame, in which one the full  $B$  occupation occurs by  $T = 400$ , after a long transient period up to  $T = 300$ .

### 4. Memory

As long as only the results from the last round are taken into account and the outcomes of previous rounds are neglected, the model considered up to now may be termed *ahistoric*, although it is not fully memoryless as there is chain (or Markovian) mechanism inherent in it, so that previous results affect further outcomes.

In the *historic* model we consider in this section, after the time-step  $T$ , for every cell  $i$ : (a) all the payoffs coming from the previous rounds are accumulated, giving  $\pi_i^{(T)}(p_i^{(1)}, \dots, p_i^{(T)}) = p_i^{(T)} + \sum_{t=1}^{T-1} \alpha^{T-t} p_i^{(t)}$ , and (b) players are featured by a

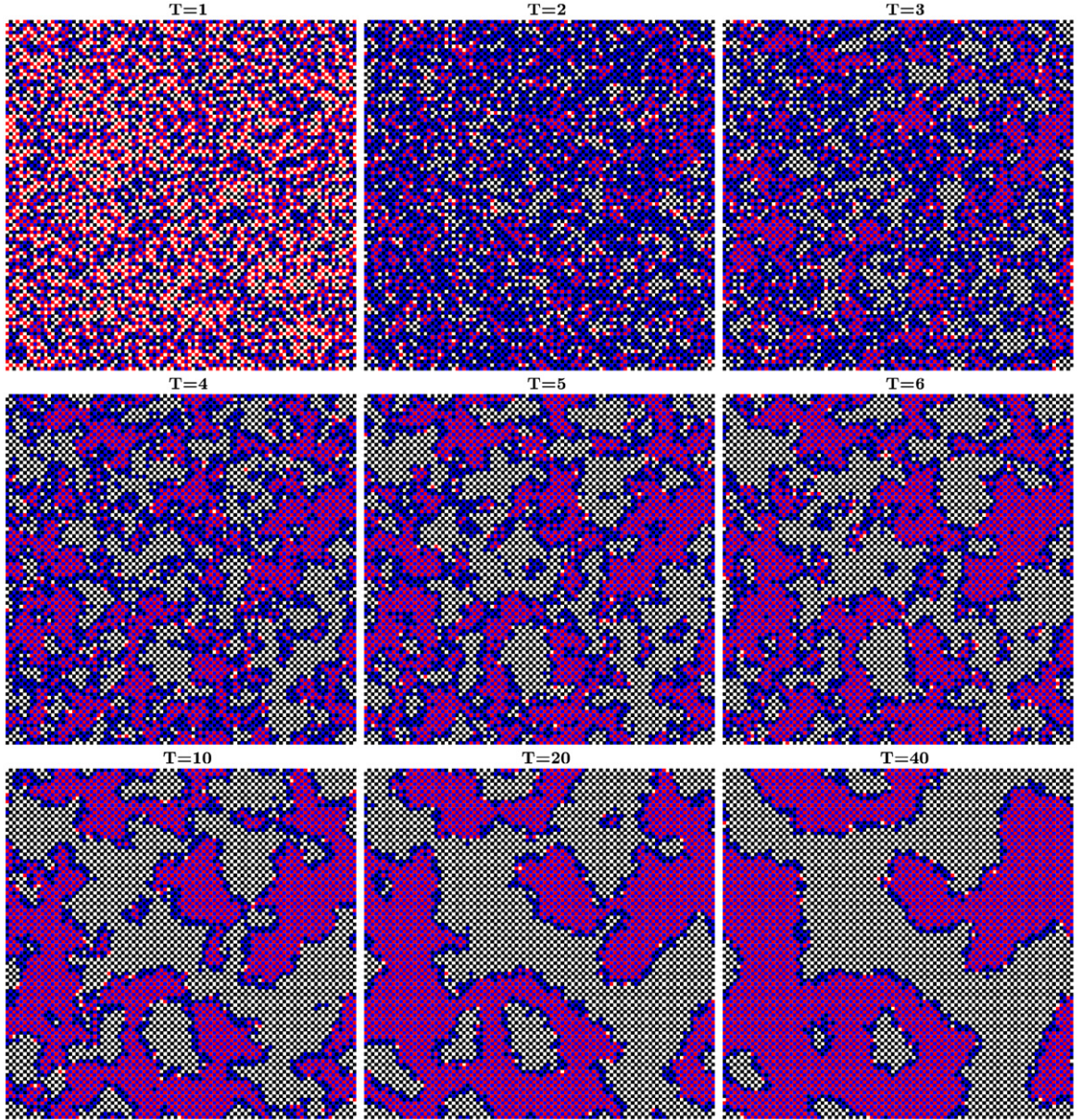


**Fig. 2.** Initial patterns in the ( $R = 5, r = 1$ ) probabilistic BOS CA in a  $100 \times 100$  lattice size. Color code: red  $\rightarrow \sigma B$ , blue  $\rightarrow \varphi B$ , black  $\rightarrow \sigma F$ , blank  $\rightarrow \varphi F$ . The color blue tends to be masked by red in the agreement clusters. (For interpretation of the references to colour in this figure legend, the reader is referred to the web version of this article.)

summary of past decisions ( $\delta_i^{(T)}$ ), not only the last one. Thus,

$$m_i^{(T)}(d_i^{(1)}, \dots, d_i^{(T)}) = \frac{d_i^{(T)} + \sum_{t=1}^{T-1} \alpha^{T-t} d_i^{(t)}}{1 + \sum_{t=1}^{T-1} \alpha^{T-t}} \equiv \frac{\omega_i^{(T)}}{\Omega^{(T)}} \Rightarrow \delta_i^{(T)} = \text{round}(m_i^{(T)}).^2$$

The choice of the *memory factor*  $0 \leq \alpha \leq 1$  simulates the remnant memory effect: the limit case  $\alpha = 1$  corresponds to equally weighted records (*full* memory model), whereas  $\alpha \ll 1$  intensifies the contribution of the most recent iterations and diminishes the contribution of the past ones (*short-term* memory); the choice  $\alpha = 0$  leads to the ahistoric model. Due to

<sup>2</sup> This geometric memory mechanism is *accumulative* in its demand for knowledge of past history:  $\pi_i^{(T)} = \alpha \pi_i^{(T-1)} + p_i^{(T)}$ ,  $\omega_i^{(T)} = \alpha \omega_i^{(T-1)} + d_i^{(T)}$ .

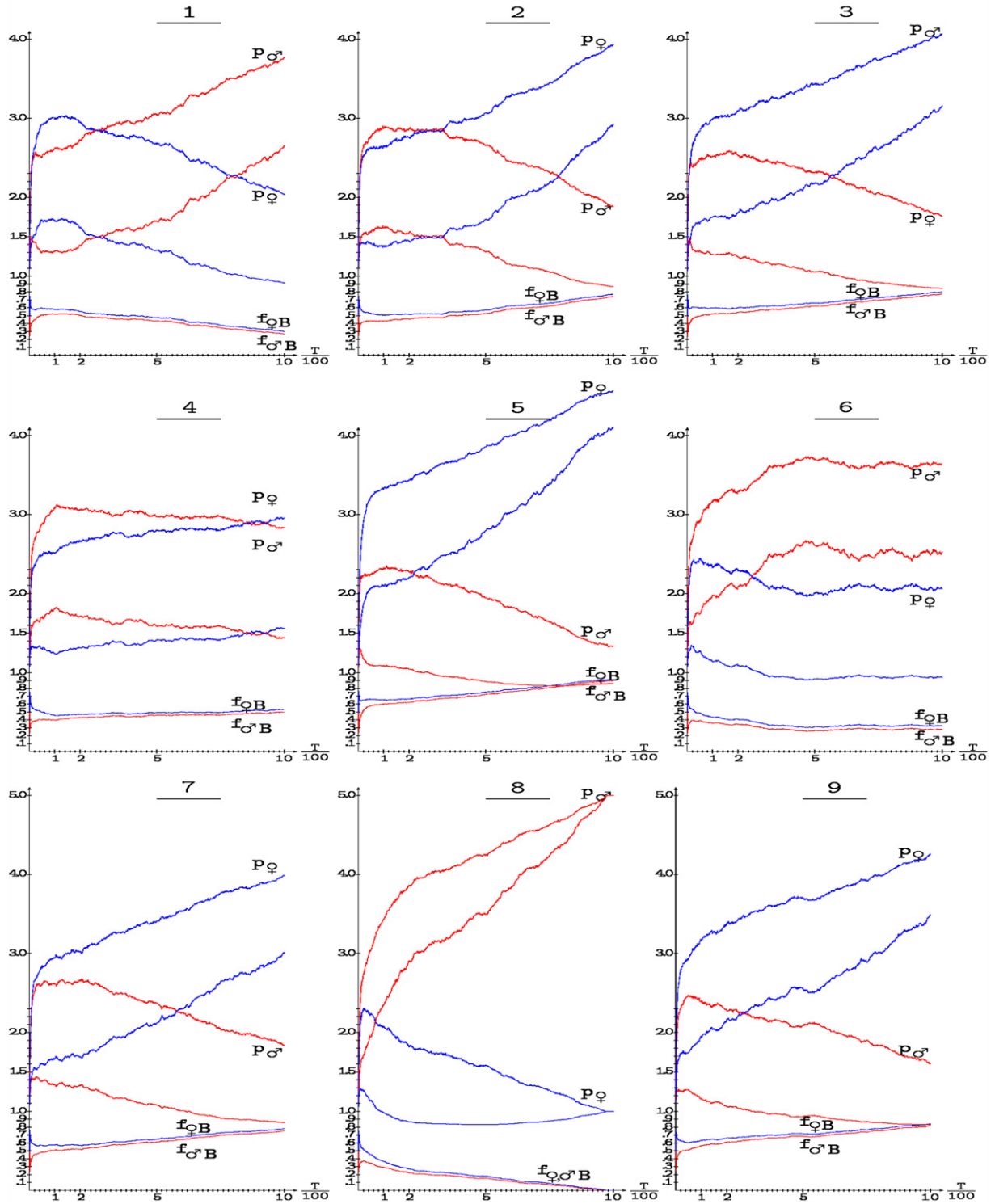


**Fig. 3.** The ballet frequency ( $f$ ) and mean payoff per encounter ( $p$ ) in nine simulations of the probabilistic (5, 1)-BOS cellular automaton. Ahistoric model.

rounding, memory of decisions is not operative if  $\alpha \leq 0.5$ , i.e.,  $\delta \equiv d$ , but memory of payoffs ( $\pi \neq p$ ) affects the dynamics even with low  $\alpha$  values.

Again, in each round or generation  $T$ , every player plays with each of his/her four partner-neighbors. In the deterministic model, the decision  $\delta^{(T)}$  in the cell of the mate neighborhood with the highest accumulated payoff ( $\pi^{(T)}$ ) will be adopted as

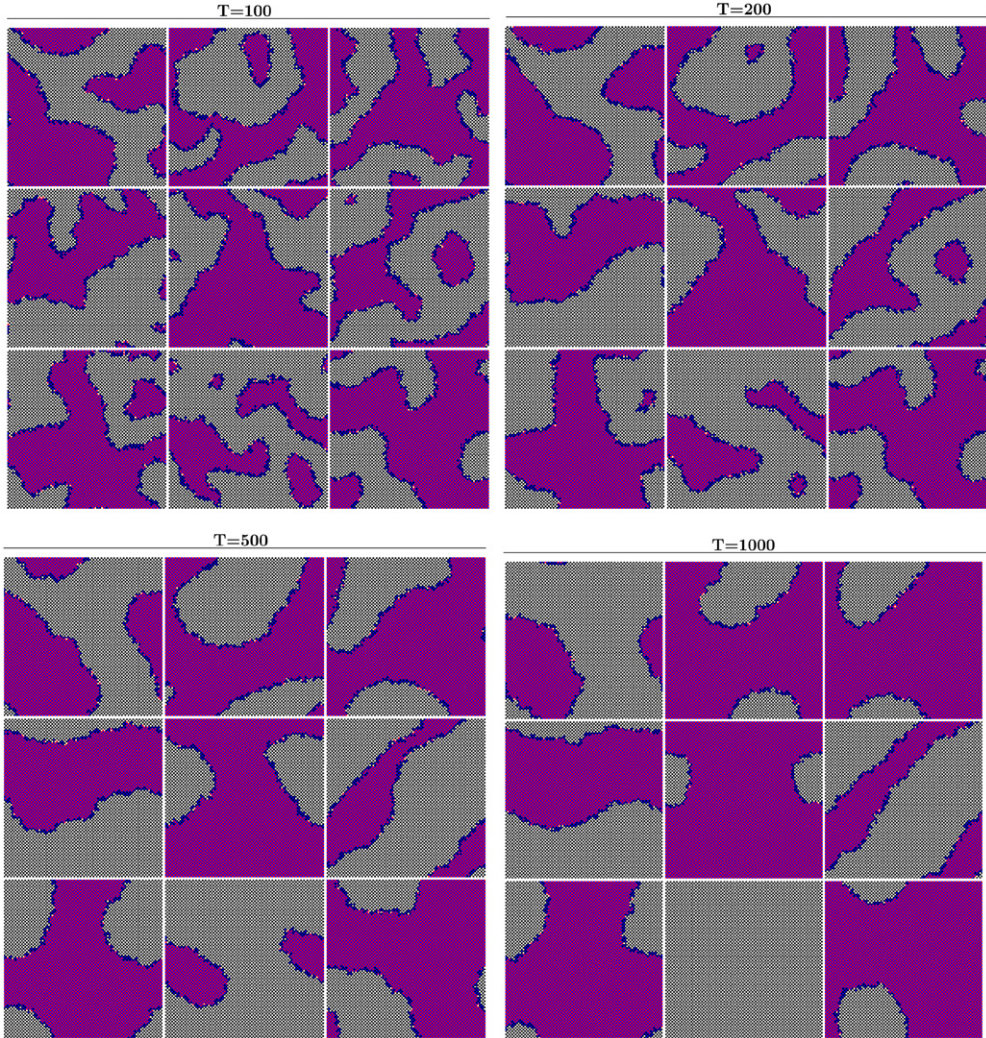


**Fig. 4.** Patterns at  $T = 100, 200, 500$  and  $1000$  in the probabilistic  $(5, 1)$ -BOS CA simulations of Fig. 3. Color code as in Fig. 2. (For interpretation of the references to colour in this figure legend, the reader is referred to the web version of this article.)

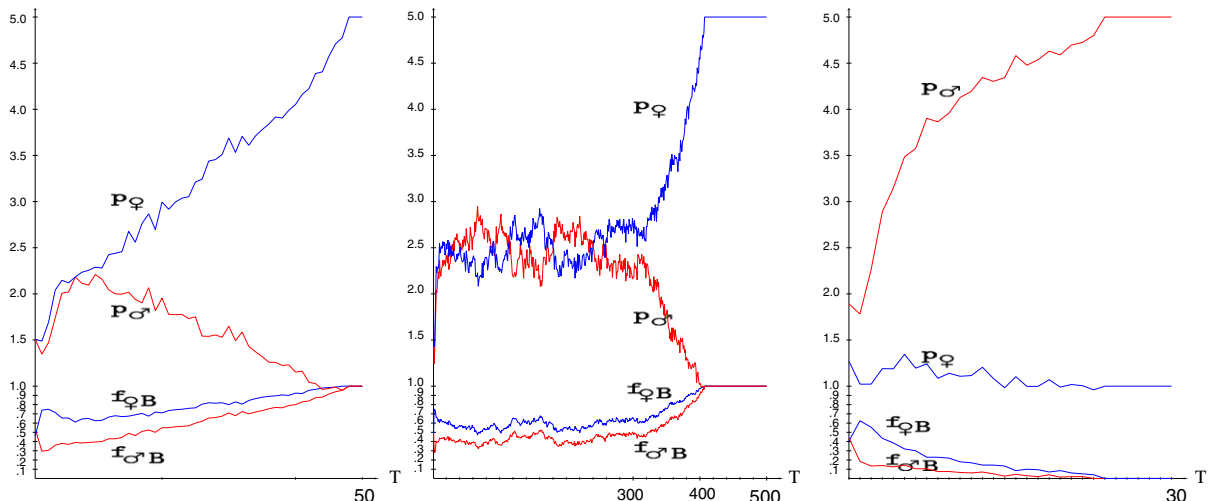


**Fig. 5.** The ballet frequency ( $f$ ) and mean payoff per encounter ( $p$ ) in a  $20 \times 20$  lattice.

the choice to play ( $d_i^{(T+1)}$ ) in the next round. The probabilistic updating scheme becomes with memory:

$$P(d_i^{(T+1)} = F) = \frac{\sum_{j \in \mathcal{N}_i / \delta_j^{(T)} = F} \pi_j^{(T)}}{\sum_{j \in \mathcal{N}_i} \pi_j^{(T)}}, \quad P(d_i^{(T+1)} = B) = 1 - P(d_i^{(T)} = F). \quad (6)$$

We have studied the effect of the kind of memory implementation considered here<sup>3</sup> in the spatialized prisoner's dilemma game in various contexts [17–19], concluding that memory notably boosts cooperation. These studies consider not only unlimited trailing memory (as done here), but the study of the effect of  $\tau$ -limited trailing memory in which:  $\pi_i^{(T)} = \pi(p_i^{(T-\tau+1)}, \dots, p_i^{(T)})$ , and  $\delta_i^{(T)} = \delta(d_i^{(T-\tau+1)}, \dots, d_i^{(T)})$ . The length of the trailing memory may be set to  $\tau = 1$  for comparison with the *ahistoric*, rather Markovian, model.  $\pi_i^{(T)} = p_i^{(T)}$ ,  $\delta_i^{(T)} = d_i^{(T)}$ , albeit.

## 5. The BOS with memory

**Fig. 6** shows the evolution of the ballet frequency and mean payoff per encounter in the nine scenarios of the probabilistic (5, 1)-BOS cellular automaton of **Fig. 3** with  $\alpha = 0.7$  memory. The inertial effect of memory induces a notable moderation in the trend of the  $f_{QB}$  and  $f_{\sigma^*B}$  parameters either to increase or decrease, thus the evolution of the frequency curves appear much more horizontal in **Fig. 6** compared to those in **Fig. 3**. In parallel with this kind of  $f$ -stabilization, there is a moderation in the way in which the mean payoffs per encounter diverge. Particularly appealing are the simulations labeled 3, 7 and 8, in which ones with the ballet frequencies are not far from 0.5, and both mean payoffs per encounter reach fairly high values.

**Fig. 7** shows the patterns at  $T = 1000$  in the nine scenarios of the probabilistic (5, 1)-BOS CA of **Fig. 3** with increasing values of the  $\alpha$  memory factor. According to the  $\alpha = 0.7$  dynamics in **Fig. 6**, the FF and BB clusters in its corresponding panel in **Fig. 7** are not so unbalanced in size as they are in the  $T = 1000$  panel in **Fig. 4**. In particular, no simulation leads to the full FF or BB occupation in the  $\alpha = 0.7$  panel of **Fig. 7**.

The inertial effect of memory is more apparent as the memory charge increases. Thus for example, the dynamics of the top-left simulation with  $\alpha = 0.7$  memory in **Fig. 6** is shown in **Fig. 8** with higher  $\alpha$  memory factor values. As a result of the effect of increasing the memory charge, i.e., the inertial effect, (i) the frequencies (of Ballet) do not recover from the initial divergence at the high degree that they recover with lower memory, and (ii) their trend to an extreme value is restrained. In parallel to that, the payoff parameters keep lower and closer. The full memory implementation turns out to be paradigmatic of the effect of memory, because the  $f$ -recovery is very small, and there is no appreciable drift to extreme values. This is much in the way as in the deterministic ahistoric simulations in **Fig. 1**, albeit with lower  $f$ -recovery, and consequently lower payoffs, in the probabilistic full memory simulation compared to the deterministic ahistoric ones.

As a rule, memory notably restrains the velocity of one-choice full occupation in small lattices. This is shown in **Fig. 9**, that departs from the same scenarios of **Fig. 5**, but implementing  $\alpha = 0.7$  memory. Thus, the  $B$ -occupation in the far left frame is reached by  $T = 180$  instead of by  $T = 50$ , and that in the far right panel is delayed from  $T = 30$  up to  $T = 60$ . In the simulation in the central frame, which resists the  $B$ -occupation already in the ahistoric model, there is no apparent lattice occupation up to  $T = 1000$ . On the contrary, both players get a high payoff up to this time-step, though it is likely that  $B$  will occupy the lattice in the very long term.

## 6. Conclusions and future work

The spatial structure enables the emergence of clusters of coincident choices in the iterated battle of the sexes game, leading to the mean payoff per encounter to values that are accessible only in the cooperative two-person game scenario, which constitutes a notable case of self-organization. With probabilistic updating of choices both kinds of players reach mean payoffs per encounter that are notably higher than those reached with a deterministic updating mechanism, albeit the evolutionary dynamics does not stabilize, and one of the two possible choices tends to prevail for both kinds of players. Memory of past payoffs and choices induces an inertial effect that moderates this tendency, so that intermediate levels of the memory charge, tend to favor fairly stable high egalitarian payoffs without impeding the necessary recovery from their initial plummeting.

As a natural extension of the binary model adopted here, the strong 0–1 assumption underlying the model can be relaxed by allowing for degrees of choices in a continuous-valued scenario. Denoting by  $x$  the degree of  $F$  choice of the  $\sigma$ -player and by  $y$  the degree of  $F$  choice of the  $\varphi$ -player, a consistent way to specify the payoff for values of  $x$  and  $y$  other than zero or one is to simply interpolate between the extreme payoffs of the binary case. Thus, the expected payoffs in the probabilistic strategies binary scenario given in the introduction, become the actual payoff in the continuous-valued context. We have

<sup>3</sup> Which differs from the usual memory implementation in spatial games, consisting in designing strategies which determine the next move of a player given the history (genome) of past moves [14,15], whereas scores are treated in a Markovian way. Probabilistic simulations with genome-type memory are implemented in [16].

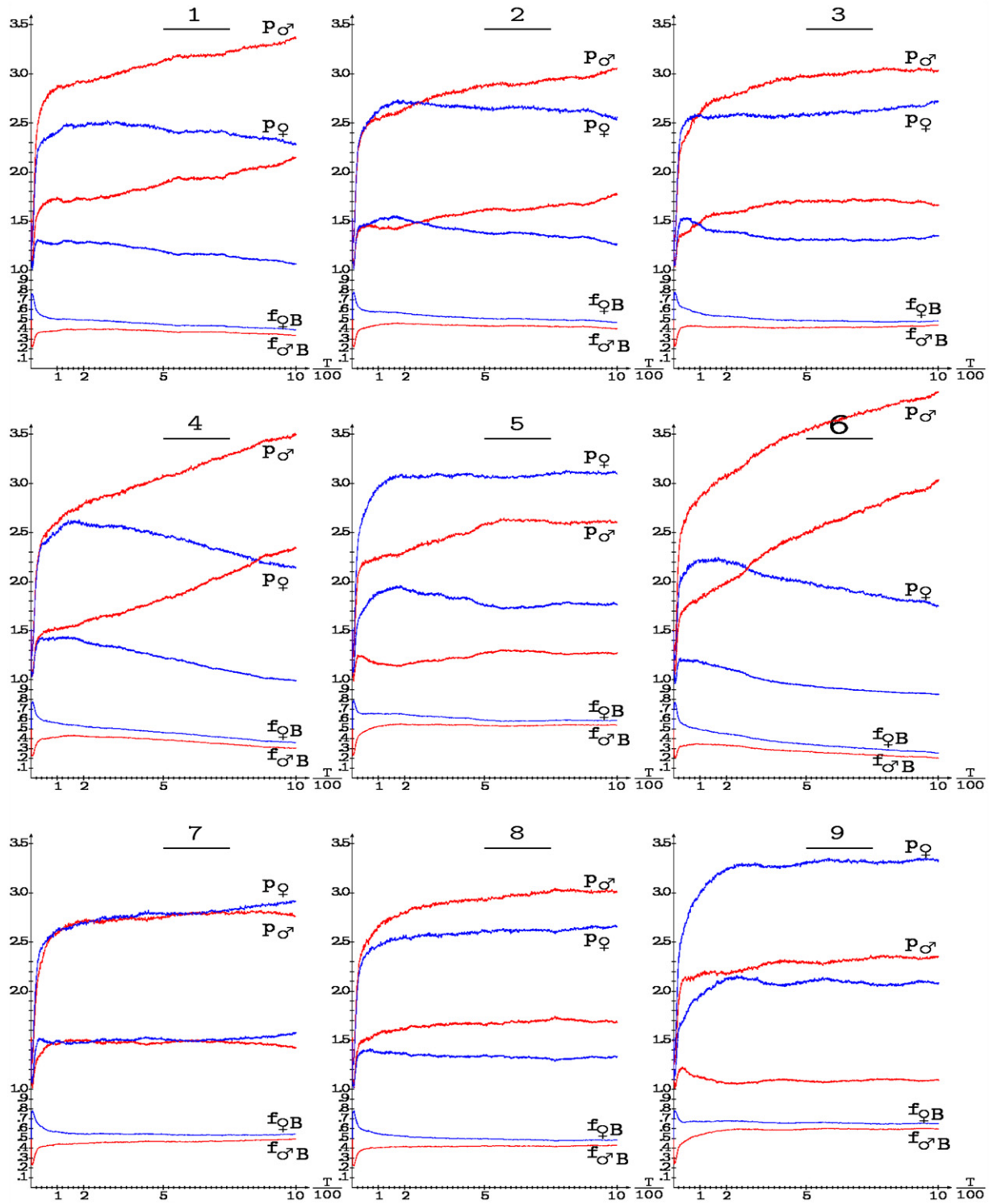


**Fig. 6.** The ballet frequency ( $f$ ) and mean payoff per encounter ( $p$ ) in the nine scenarios of the probabilistic (5, 1)-BOS cellular automaton of Fig. 3 with  $\alpha = 0.7$  memory.

studied such an approach dealing with the spatialized PD game [20,18], and we plan to implement it in the battle of the sexes game in the near future.

In real-life situations the preferential choice and refusal of partners plays an important role in the emergence of cooperation [21]. We have studied the effect of memory on a simple, deterministic, structurally dynamic PD game, in which

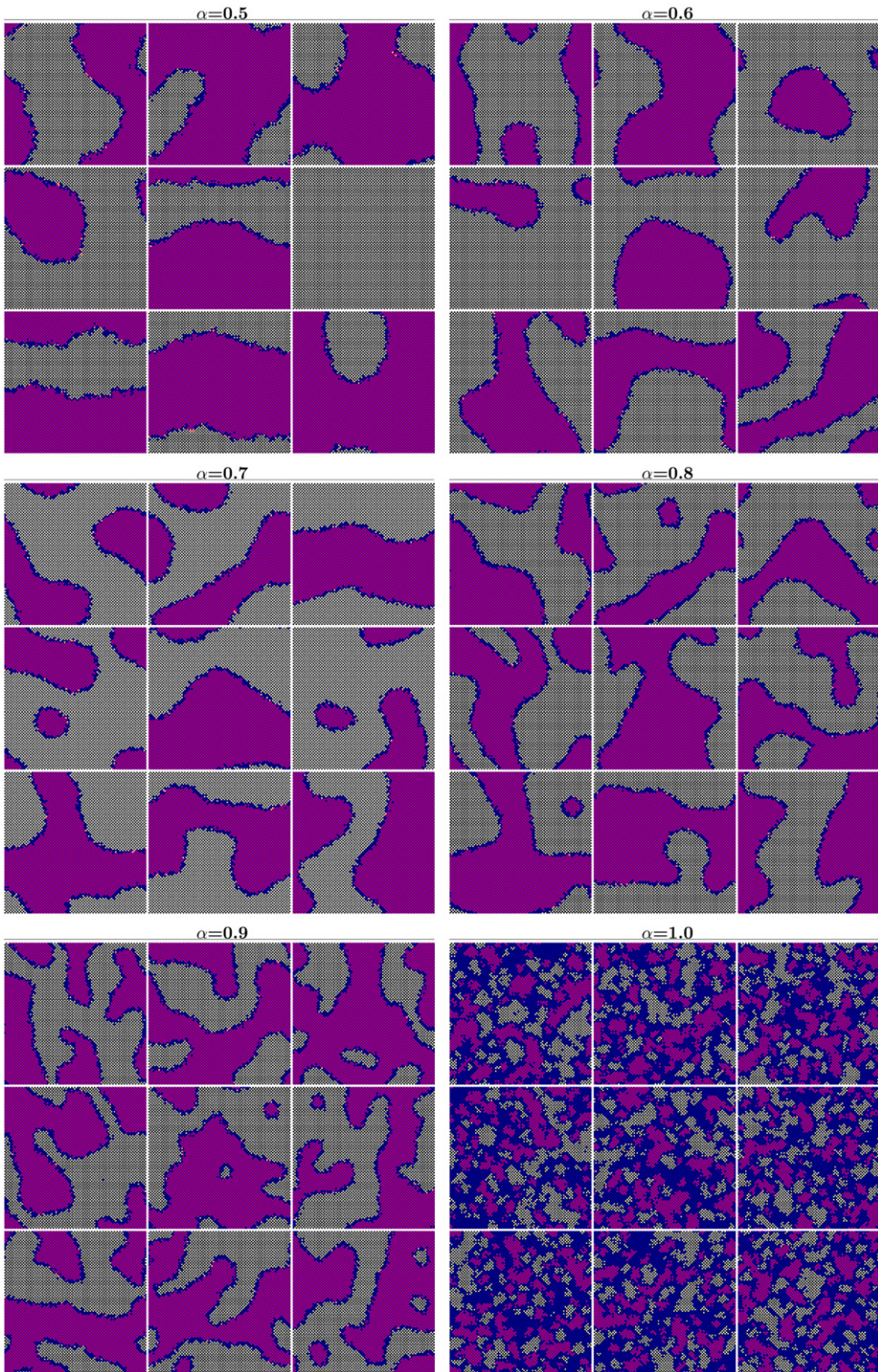


**Fig. 7.** Patterns at  $T = 1000$  in the nine scenarios of the probabilistic (5, 1)-BOS CA of Fig. 3 with increasing values of the  $\alpha$  memory factor. (For interpretation of the references to colour in this figure legend, the reader is referred to the web version of this article.)

state and link configurations are *both* dynamic and are continually interacting [22]. Further study is due on the structurally dynamic battle of the sexes. The study of the effect of memory in other structurally spatialized games, as well as in games on networks [17] is also planned as a future work.

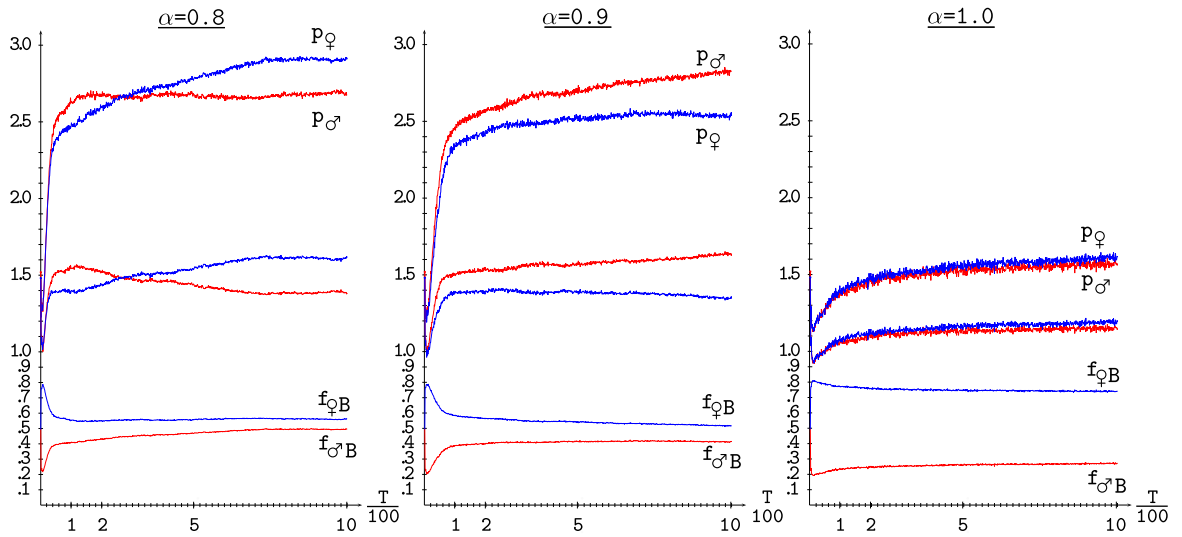


**Fig. 8.** The  $B$ -frequency ( $f$ ) and mean payoff per encounter ( $p$ ) with high  $\alpha$ -memory.

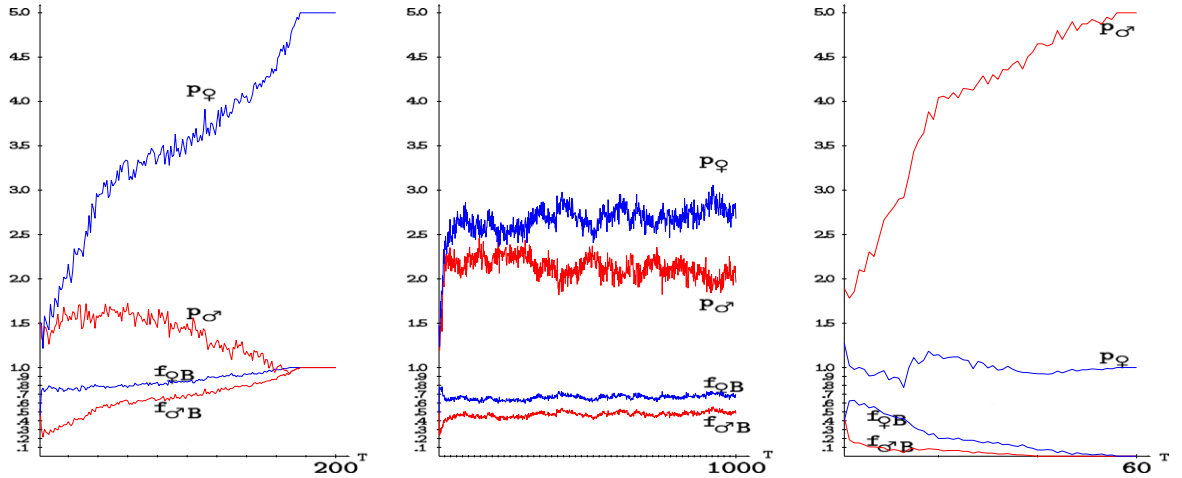


**Fig. 9.** The ballet frequency ( $f$ ) and mean payoff per encounter ( $p$ ) in a  $20 \times 20$  lattice with  $\alpha = 0.7$  memory.

Last but not least, asynchronous updating, as well as the effect of increasing degrees of spatial dismantling (via rewiring for example, as done in [20] in the PD context), which would lead to more realistic models, are tasks left to be scrutinized in further studies.

## Acknowledgment

This work was supported under Spanish grant no. MTM2009-14621-C02-02.

## References

- [1] J. Hofbauer, K. Sigmund, *Evolutionary Games and Population Dynamics*, Cambridge University Press, 2003.
- [2] J. Maynard-Smith, *Evolution and the Theory of Games*, Cambridge University Press, 1982.
- [3] G. Owen, *Game Theory*, Academic Press, 1995.
- [4] R.J. Aumann, Subjectivity and correlation in randomized strategies, *J. Math. Econom.* 1 (1974) 67–96.
- [5] R.J. Aumann, Correlated equilibrium as an expression of Bayesian rationality, *Econometrica* 55 (1) (1987) 1–18.
- [6] J. Eisert, M. Wilkens, M. Lewenstein, Quantum games and quantum strategies, *Phys. Rev. Lett.* 83 (15) (1999) 3077–3080.
- [7] P. Frackiewicz, The ultimate solution to the quantum battle of the sexes game, *J. Phys. A: Math. Gen.* 42 (36) (2009) 365305.
- [8] A. Nawaz, A.H. Toor, Dilemma and quantum battle of sexes, *J. Phys. A: Math. Gen.* 37 (15) (2004) 4437–4443.
- [9] N.M. Nowak, R.M. May, Evolutionary games and spatial chaos, *Nature* 359 (1992) 826–829.
- [10] M.A. Nowak, M. May, The spatial dilemmas of evolution, *Int. J. Bifurcation Chaos* 3 (11) (1993) 35–78.
- [11] R. Axelrod, *The Evolution of Cooperation*: Revised Edition, Basic Books, 2008.
- [12] J. Zhao, N. Szilagyi, F. Szidarovsky, An  $n$ -person battle of sexes game, *Physica A* 387 (2008) 3669–3677.

- [13] J. Zhao, N. Szilagyi, F. Szidarovsky, An  $n$ -person battle of sexes game—a simulation study, *Physica A* 387 (2008) 3668–3788.
- [14] K. Lindgren, M.G. Nordahl, Evolutionary dynamics of spatial games, *Physica D* 75 (1994) 292–309.
- [15] K. Lindgren, M.G. Nordahl, Cooperation and community structure in artificial ecosystems, in: C. Langton (Ed.), *Artificial Life*, The MIT Press, 1995, pp. 16–37.
- [16] C. Hauert, H.G. Schuster, Effect of increasing the number of players and memory steps in the iterated prisoner's dilemma, a numerical approach, *Proc. R. Soc. Lond. Ser. B* 264 (1997) 513.
- [17] R. Alonso-Sanz, Spatial order prevails over memory in boosting cooperation in the iterated prisoner's dilemma, *Chaos* 19 (2) (2009) 023102.
- [18] R. Alonso-Sanz, M.-C. Martin, M. Martin, The effect of memory in the spatial continuous-valued prisoner's dilemma, *Internat. J. Bifur. Chaos* 11 (8) (2001) 2061–2083, and the references therein.
- [19] R. Alonso-Sanz, M. Martin, Memory boosts cooperation, *Internat. J. Modern Phys. C* 17 (6) (2005) 841–852.
- [20] R. Alonso-Sanz, Memory versus spatial disorder in the support of cooperation, *Biosystems* 97 (2009) 90–102.
- [21] G. Szabo, G. Fáth, Evolutionary games on graphs, *Phys. Rep.* 446 (2007) 97–216.
- [22] R. Alonso-Sanz, Memory boosts cooperation in the structurally dynamic prisoner's dilemma, *Internat. J. Bifur. Chaos* 19 (9) (2009) 2899–2926.